

Negative-parity states near the yrast line in ^{144}Nd

J.K. Jewell, O.J. Tekyi-Mensah, P.D. Cottle, J. Döring,
 P.V. Green, J.W. Holcomb,* G.D. Johns, T.D. Johnson,† K.W. Kemper,
 P.L. Kerr, S.L. Tabor, P.C. Womble,‡ and V.A. Wood
Department of Physics, Florida State University, Tallahassee, Florida 32306-3016
 (Received 17 January 1995; revised manuscript received 8 June 1995)

The near-yrast spectrum of the $N=84$ isotope ^{144}Nd has been studied using the $^{130}\text{Te}(^{18}\text{O},4n)$ reaction at a lab energy of 85 MeV and the techniques of γ -ray spectroscopy. Sixteen new states and 23 new γ rays were placed in the level scheme. Most of the yrast and near-yrast negative-parity states have been interpreted in terms of empirical shell-model configurations. However, the interpretation of a sequence of states from $J=17-24$ in terms of the $h_{11/2}^3 g_{7/2}^{-1} d_{5/2}^{-6}$ proton configuration is problematic because the observed energies cannot be satisfactorily reproduced with empirical shell-model calculations.

PACS number(s): 23.20.Lv, 21.60.Cs, 23.20.En, 27.60.+j

I. INTRODUCTION

The nucleus ^{146}Gd , with its closed major shell of 82 neutrons and closed subshell of 64 protons, is considered one of the best examples of a spherical nucleus in the Periodic Table. Since ^{146}Gd and the adjacent nuclei are neutron deficient, they have offered excellent opportunities for studying shell-model structures at high angular momenta via fusion-evaporation reactions. It has been demonstrated in several cases (including ^{145}Pm [1]) that high-spin states of nuclei with neutron and proton numbers which are both several nucleons removed from the closed $N=82$ and $Z=64$ (sub)shells can also be described in terms of the spherical shell model.

In this article we present a study of high-spin states of ^{144}Nd , which has four protons less and two neutrons more than ^{146}Gd . The level scheme we deduced includes 16 new states and 23 new γ rays compared to the previous studies [2,3], and extends up to $J=24$ and an energy of 8.9 MeV. In addition, we compare the experimental results to calculations using an empirical shell model, in which interaction energies from neighboring nuclei are used. These calculations demonstrate that the shell model is a useful tool for understanding high-spin structure even in a nucleus so far away from ^{146}Gd . A preliminary report was given in [4].

II. EXPERIMENTAL PROCEDURE

The nucleus ^{144}Nd was produced with the $^{130}\text{Te}(^{18}\text{O},4n)$ fusion evaporation reaction with a thick (500 mg/cm²) target

isotopically enriched to 99% and with a beam energy of 85 MeV. This beam energy was chosen to optimize the study of ^{143}Nd ; however, substantial data were obtained on ^{144}Nd as well because a thick target was used. The beam was produced by the Florida State University FN Tandem Van de Graaff and Superconducting Linear Accelerators. Prompt γ - γ coincidences were detected with the Florida State University-University of Pittsburgh array. For this experiment, the array consisted of nine Compton-suppressed Ge γ -ray detectors, each of approximately 25% relative efficiency. Five of the detectors were placed at 90° relative to the beam, two at 35° and two at 145°, allowing the measurement of directional correlations from oriented states (DCO) ratios for determinations of transition multipolarities. Approximately 4.5×10^8 coincidence events were collected.

To construct the level scheme, all of the twofold coincidence events were sorted into a triangular matrix. Background-subtracted coincidence spectra were then projected and used to determine coincidence relationships. The DCO ratios were determined from coincidence events between the 90° detectors and the detectors at either 35° or 145°. These events were sorted into a square matrix in which one axis corresponded to the 90° energy and the other to the 35° or 145° energy. The DCO ratio for a γ ray γ_1 was calculated from the observed intensities I using the relation

$$R_{\text{DCO}} = \frac{I(\gamma_1 \text{ observed at } 35^\circ \text{ and } 145^\circ, \text{ gated by } \gamma_G \text{ observed at } 90^\circ)}{I(\gamma_1 \text{ observed at } 90^\circ, \text{ gated by } \gamma_G \text{ observed at } 35^\circ \text{ and } 145^\circ)} \quad (1)$$

*Present address: Martin Marietta Information Systems, Orlando, FL 32828.

†Present address: Physics Department, University of Notre Dame, Notre Dame, IN 46556.

‡Present address: Oak Ridge National Laboratory, Oak Ridge, TN 37831.

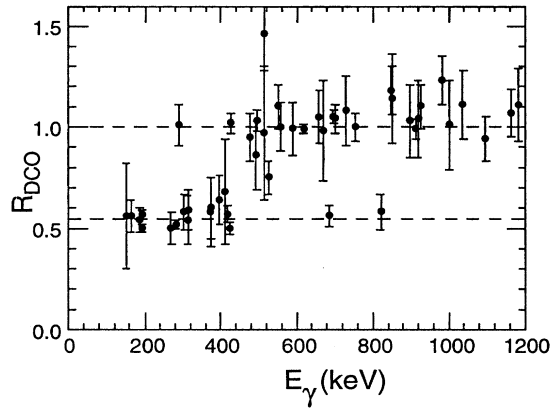


FIG. 1. DCO ratios measured for ^{144}Nd in the present experiment.

Well-known stretched $E2$ transitions were used as the gating transitions γ_G . In all cases the DCO results from several gating transitions were compared to determine an average and to estimate an uncertainty. For stretched $E2$ transitions, the DCO ratios are 1.0. The ratios for pure, stretched dipole transitions (either $M1$ or $E1$) from states of angular momentum greater than $10\hbar$ are near 0.55 for values of the alignment $\sigma/J_i \approx 0.25$, which is suggested by a previous study of the neighboring nuclei $^{144,145}\text{Pm}$ [1] using a similar beam-target combination ($^{19}\text{F} + ^{130}\text{Te}$). For the expression σ/J , the alignment of the magnetic substates is assumed to follow a Gaussian distribution with width σ , and J is the spin of the state. While mixed transitions, particularly $M1/E2$ transitions, may occur, nearly all of the DCO ratios for γ rays placed in ^{144}Nd are consistent with values of 1.0 or 0.55. This is illustrated in Fig. 1. The DCO ratios and intensities of the γ rays are compiled in Table I.

We attempted a study of the angular distributions of γ rays in ^{144}Nd at 85 MeV. Angular distributions for ^{144}Nd had been studied previously using the same beam-target combination at 70 MeV [2]. We were not able to extract any new angular distribution information because the new γ rays we placed in the present level scheme were too weak to be seen cleanly enough in the singles spectrum to be reliably fit with Gaussian peak-fitting programs. Furthermore, at 85 MeV, doublets (probably from $^{142,143}\text{Nd}$) obscured γ rays from ^{144}Nd that are clean at 70 MeV.

III. LEVEL SCHEME AND J^π ASSIGNMENTS

The level scheme deduced in the present study is shown in Fig. 2. There are several changes from the level scheme given in our preliminary report [4]. The quality of the coincidence data used to build the level scheme is illustrated in Figs. 3 and 4.

The spin and parity assignments listed for states up to 4936 keV are taken from [3], in which conversion electron measurements have been reported and used in conjunction with γ ray angular distribution data from Ref. [2] to make assignments. For all the states above 5.24 MeV (which were reported for the first time in our preliminary paper [4]), spin assignments are made on the basis of DCO ratios. The spin

TABLE I. Properties of γ rays observed in ^{144}Nd .

E_γ (keV) ^a	E_i (keV) ^a	I_γ ^b	R_{DCO}	Multipolarity
96.6	2709.3	3(2)	0.48(13)	$M1$
150.8	7965.4	3(1)	0.56(26)	($M1$)
155.1	4064.8	0.5(1)	c	
162.2	4623.2	10(1)	0.56(8)	$M1$
185.7	3672.2	7(2)	0.54(6)	($M1$)
193.1	2902.4	17(1)	0.50(2)	$E1$
193.7	4935.7	6(1)	0.57(2)	($M1$)
236.0	4064.8	1.0(5)	c	
268.9	7814.5	4(2)	0.50(8)	($M1$)
269.3	4623.2	2(1)	c	
281.3	4742.0	5(1)	0.52(2)	$M1$
290.4	2902.4	2(1)	1.01(10)	$E2$
302.2	5238.0	12(1)	0.58(9)	($M1$)
309.2	4353.8	4(1)	0.61(6)	($M1/E2$)
312.6	4935.7	7(1)	0.54(12)	($M1$)
314.6	5552.7	30(6)	0.59(10)	($M1$)
315.0	6963.5	4(2)	c	
357.1	3233.1	2(1)	c	
373.0	4045.1	18(2)	0.58(17)	($E1$)
373.4	7376.2	14(1)	0.60(15)	($M1$)
392.8	4064.8	5(1)	0.46(21)	($M1$)
396.1	4460.9	13(2)	0.64(12)	$M1/E2$
409.8	5962.5	12(5)	0.68(26)	($M1$)
415.9	4460.9	14(1)	0.57(4)	$M1$
423.6	3909.9	5(2)	0.65(11)	($E1$)
423.7	3395.5	25(8)	0.50(3)	$E1$
426.9	2217.6	27(1)	1.02(5)	$M1/E2$
476.9	1790.7	84(6)	0.95(12)	$E2$
493.7	5966.0	20(4)	0.86(17)	($E2$)
494.2	3395.5	11(4)	1.03(5)	$M1/E2$
514.4	3486.5	6(1)	0.97(33)	$M1/E2$
525.0	4353.8	3(1)	0.75(8)	
551.0	4460.9	5(2)	1.10(11)	($E2$)
558.4	4623.2	20(4)	1.00(12)	$E2$
610.7	3486.5	2(1)	c	
614.9	5238.0	11(1)	c	
617.0 ^d	5552.7	7(3)	c	
618.2	1313.8	93(5)	0.99(2)	$E2$
658.4	2876.0	6(1)	1.05(13)	($E2$)
669.4	4064.8	29(3)	0.98(25)	$E2$
676.8	3909.9	1.0(5)	c	($E2$)
677.0	4742.0	11(1)	1.11(7)	($E2$)
686.1	3395.5	4(1)	0.56(5)	$E1$
686.2	6648.7	1.0(5)	c	($M1$)
695.6	695.6	100 ^e	1.05(3)	$E2$
700.4	3672.2	12(7)	1.04(7)	($E2$)
722.4	5962.5	8(4)	1.13(6)	($E2$)
729.8	5471.8	10(1)	1.08(17)	($E2$)
754.3	2971.9	25(2)	1.00(7)	$E2$
821.3	2612.0	8(2)	0.58(9)	$E1$
849.1	5471.8	9(1)	1.18(12)	($E2$)
851.0	7814.5	6(2)	1.14(22)	($E2$)
896.7	7545.4	7(1)	1.03(18)	($E2$)
913.2	4742.0	8(1)	0.99(5)	$E2$
918.6	2709.3	40(4)	1.04(19)	$E2$

TABLE I. (Continued).

E_γ (keV) ^a	E_i (keV) ^a	I_γ ^b	R_{DCO}	Multipolarity
926.4	3828.8	15(1)	1.10(11)	$E2$
980.8	8946.1	12(8)	1.23(12)	($E2$)
1001.0	6963.5	5(2)	1.01(22)	($E2$)
1036.8	7002.8	22(4)	1.11(17)	($E2$)
1096.0	6648.7	5(1)	0.94(11)	($E2$)
1161.9	4064.8	7(1)	1.07(12)	$E2$
1180.6	2971.9	20(3)	1.11(18)	$E2$

^aUncertainties on energies are 0.2 keV.

^bNormalized so that $I_\gamma=100$ for the 695.6 keV γ ray.

^cNo useful DCO ratio could be extracted.

^dTransition tentatively placed in level scheme.

^eUsed for normalizing intensities.

assignments for states up to 7.965 MeV are established by several pathways; therefore, we have confidence in these assignments. The primary reservation we have about these assignments concerns our assumption that a transition with a DCO ratio of 1.0 is a stretched quadrupole transition. Mixed $M1/E2$ transitions can also have DCO ratios of 1.0 for certain values of the mixing ratio δ . However, a significant admixture of $E2$ would be necessary to give such a DCO ratio. Because $E2$ transitions are generally weak in these spherical nuclei, it is unlikely that this occurs. However, the possibility cannot be dismissed.

We have suggested negative parity for the states above 5.24 MeV because they directly feed only negative-parity states in the lower part of the level scheme. It is not possible

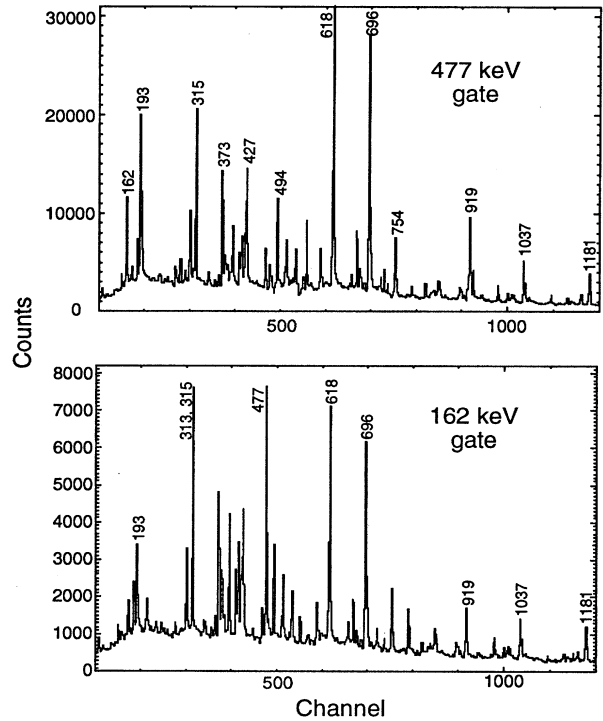


FIG. 3. Gamma-ray coincidence spectra gated on the $6^+ \rightarrow 4^+$ 477 and $13^- \rightarrow 12^-$ 162 keV transitions.

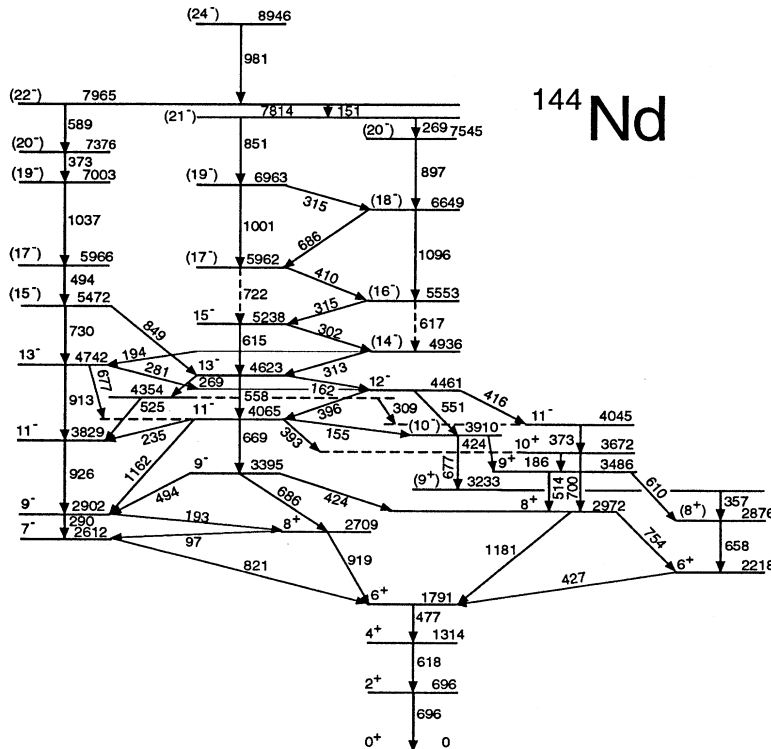


FIG. 2. Level scheme of ^{144}Nd deduced in the present work.

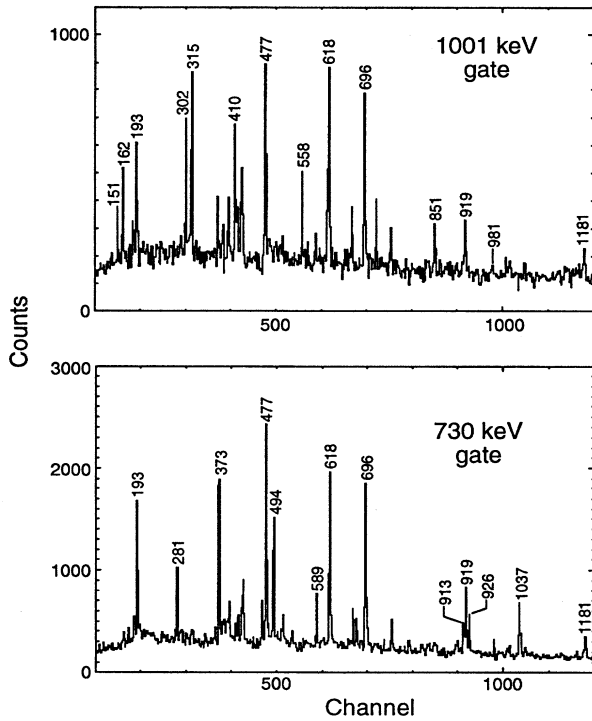


FIG. 4. Gamma-ray coincidence spectra gated on the $(19^-) \rightarrow (17^-)$ 1001 keV and $(15^-) \rightarrow 13^-$ 730 keV transitions.

to extract conversion electron coefficients for the transitions from states above 5.24 MeV in a single electron measurement because of the complexity of the spectrum.

The largest change made to the level scheme from [4] is the removal of the levels at 3388, 3574, and 4088 keV, and the placement of new levels at 3486, 3672, and 4045 keV using the same set of γ rays. These levels now match those given in [5]. The spin and parity assignments given in the present level scheme for these states are supported by the DCO ratios measured here, the electron conversion coefficients reported in [3], and the γ ray angular distribution results given in [2]. There is one remaining discrepancy between the level schemes given here and in [5]: we list negative parity for the $J=12$ state at 4461 keV, and positive parity is given in [5]. However, conversion electron results given in [3] support the negative parity assignment given here.

Several other minor changes have been made to the level scheme from [4]. Several new transitions linking states below 5 MeV have been added. In addition, an $E2$ transition linking the 5238 and 5962 keV states has been tentatively added. While the coincidence spectra support the placement of this transition, the energy measured for the transition disagrees with the difference between the energies of the levels by 2 keV. Elsewhere in our level scheme, the agreement is always better than 0.3 keV. A level which was given at 9415 keV in [4] has been removed, and a level which was tentatively placed at 5157 keV in [4] has also been removed.

TABLE II. Experimental single-particle energies used in the empirical shell-model calculations.

Nucleus	Orbit	Single-particle energy (keV)
^{145}Eu	$\pi 2d_{5/2}^{-1}$	5366
^{145}Eu	$\pi 1g_{7/2}^{-1}$	5696
^{147}Tb	$\pi 1h_{11/2}$	-1906
^{147}Gd	$\nu 2f_{7/2}$	-7339
^{147}Gd	$\nu 1i_{13/2}$	-6342

IV. EMPIRICAL SHELL-MODEL CALCULATIONS

To test the interpretation of some of the negative-parity states in ^{144}Nd , we performed empirical shell-model calculations similar to those suggested by Talmi [6]. Empirical shell-model calculations allow the decomposition of a shell model configuration into substructures corresponding to specific levels in neighboring nuclei, from which empirical interaction energies are extracted. Such calculations have been performed for a number of nuclei in the vicinity of ^{146}Gd (for example see [1,7–10]). The energy $E(\Psi, N)$ of a state Ψ in a nucleus N relative to a closed core (^{146}Gd in this case), is expressed in terms of the single-particle energies $E_{\text{sp}}(\Psi, N)$ and interaction energies $\langle(\Psi, N)\rangle$ by

$$E(\Psi, N) = E_{\text{sp}}(\Psi, N) + \langle(\Psi, N)\rangle. \quad (2)$$

To express $E(\Psi, N)$ as an excitation energy $E_x(\Psi, N)$ in the nucleus N , the ground-state energy of the nucleus $E_{\text{g.s.}}(N)$ relative to the ^{146}Gd core must be subtracted:

$$E_x(\Psi, N) = E(\Psi, N) - [E_{\text{g.s.}}(\Psi, N) - E_{\text{g.s.}}(^{146}\text{Gd})]. \quad (3)$$

Empirical single-particle energies, which are compiled in Table II, were obtained from the one-valence particle nuclei adjacent to ^{146}Gd in the following ways. The energies of the $\pi d_{5/2}^{-1}$ and $\pi g_{7/2}^{-1}$ holes are taken from ^{145}Eu states seen in proton transfer reactions [11–13]. An $11/2^-$ state was identified at 51 keV in α - γ coincidence measurements from the decay of ^{151}Ho and interpreted as the $\pi h_{11/2}$ single proton state [14]. The $h_{9/2}$ and $i_{13/2}$ neutron states in ^{147}Gd are established through decay studies of ^{147}Tb [15] and fusion-evaporation studies [16]. The 997 keV $13/2^+$ state in ^{147}Gd is a mixture of the $\nu i_{13/2}$ single-neutron configuration and the particle-octupole vibration-coupled $[\nu f_{7/2} \otimes 3^-]_{13/2}^+$ configuration. Therefore, the energy listed in Table II for the $i_{13/2}$ single neutron energy is not the energy of a pure $\nu i_{13/2}$ single-particle state. Instead, it is an effective energy, which implicitly assumes that similar admixtures of $[\nu f_{7/2} \otimes 3^-]_{13/2}^-$ occur in nuclei throughout the neighborhood of ^{146}Gd .

In the empirical shell model, the energy of the interaction between the single particles involved in a particular configuration is calculated by decomposing the interaction into terms, or multiparticle matrix elements (MPME's), which can be determined by examining the spectra of nearby nuclei. While a complete decomposition of the interaction energy of a configuration into two-body matrix elements is always possible, it is often more advantageous to decompose it

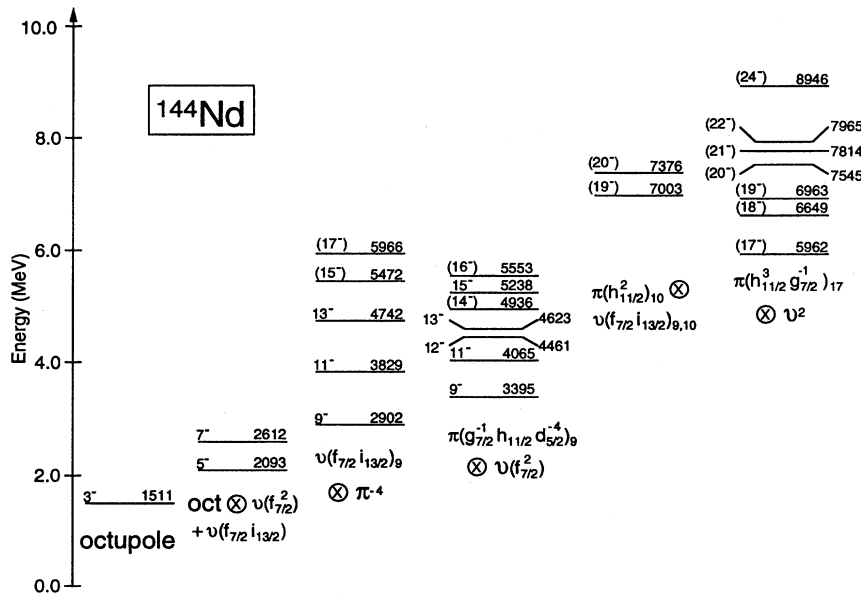


FIG. 5. Structure assignments for yrast and near-yrast negative-parity states in ^{144}Nd . The energies of several states have been taken from [17].

into MPME's representing the interaction between *more* than two particles. The MPME's are generally more closely related to the final configuration than two-body matrix elements are, and effects such as configuration mixing and core polarization are included automatically. In some cases the data needed to determine MPME's for the present calculations were not available, and in some of those cases MPME's were calculated from the two-body matrix elements which have been compiled in [8,9]. These calculations do not take configuration mixing into account explicitly. The results of these calculations are included in the discussion in Sec. V.

V. NEGATIVE-PARITY STATES NEAR THE YRAST LINE

Negative-parity states near the yrast line in ^{144}Nd can be grouped into sets of states with related structures as shown in Fig. 5. The lowest 5^- and 7^- states are 582 and 1101 keV above the octupole 3^- state, respectively. These relative energies are similar to the energies of the 2_1^+ and 4_1^+ states (696 and 1314 keV, respectively), suggesting that the lowest 5^- and 7^- states arise from the coupling of the octupole state to the 2_1^+ and 4_1^+ states. The transitions between these states could not be observed in the present experiment because the intensity in the 7^- state is taken entirely by the 821 keV $E1$ transition to the 6_1^+ state. This transition probably has a reduced matrix element $B(E1) \approx 10^{-3}$ Weisskopf unit (W.u.) ($E1$ transitions deexciting the 1511 keV 3^- state and 2093 keV 5^- state have recently been measured [18] to have $B(E1)$ values near 10^{-3} W.u.). Robinson *et al.* [18] recently reported a measurement of the reduced matrix element of the transition between the 5^- state at 2093 keV and the octupole 3^- state via the lifetime of the 5^- state. Their result, $B(E2) = 20_{-10}^{+12}$ W.u. is consistent with an interpretation of the 5^- state in terms of $2_1^+ \otimes 3_1^-$ structure.

However, it is unlikely that the 5^- and 7^- states are simple quadrupole-octupole coupled states. It was proposed by Cottle *et al.* [19] on the basis of data on inelastic proton scattering to the 5^- state that this state has a large ($\geq 50\%$)

contribution from the $\nu(f_{7/2} i_{13/2})_5$ two-quasiparticle configuration. Robinson *et al.* [18] agreed with this result, pointing out that the lower error bounds on the $E2$ and $E3$ decays from the 5^- state that they had measured were consistent with a $2_1^+ \otimes 3_1^-$ component as small as 40% of the wave function. It can be concluded from these data that 40–50% of the wave function of the 2093 keV state is $2_1^+ \otimes 3_1^-$, and 50–60% is the two-quasiparticle $\nu(f_{7/2} i_{13/2})$ configuration. While no similar lifetime and scattering data are available for the 7^- state, it is not unreasonable to expect that the wave function of this state is a mixture of the corresponding $4_1^+ \otimes 3_1^-$ and $\nu(f_{7/2} i_{13/2})_7$ configurations.

The 9^- state at 2902 keV decays via an $E2$ transition to the 7^- state at 2612 keV, and this suggests a relationship in the structure of the two states. However, the energy of this 9^- state relative to the octupole 3^- state is 1391 keV, which is significantly different than the 1791 keV energy of the 6_1^+ state. While the interaction of the octupole phonon with single particle orbits can perturb the energy of a state from the simple weak coupling prediction [$E(3_1^-) + E(6_1^+)$], a relatively pure $\nu(f_{7/2} i_{13/2})_9$ configuration should also be considered. As shown in Fig. 6, the empirical shell-model calculation for the $\nu(f_{7/2} i_{13/2})_9$ configuration yields an energy of 2976 keV, and therefore satisfactorily reproduces the experimental result.

The sequence of states up to $J=17$ (3829, 4742, 5472, and 5966 keV) which decays via a cascade of $E2$ transitions to the 2902 keV 9^- state can be interpreted as excitations of the ^{142}Nd closed neutron shell core coupled to the $\nu(f_{7/2} i_{13/2})_9$ two-neutron configuration. Empirical shell-model calculations which assume this configuration yield the satisfactory results illustrated in Fig. 6. For each of the states in this sequence the calculation reproduces the experimental result to within 260 keV.

Another 9^- state is observed at 3395 keV, and is connected by a cascade of strong $M1$ and $E2$ transitions to a sequence of states including those at 4065, 4461, 4623, 4936,

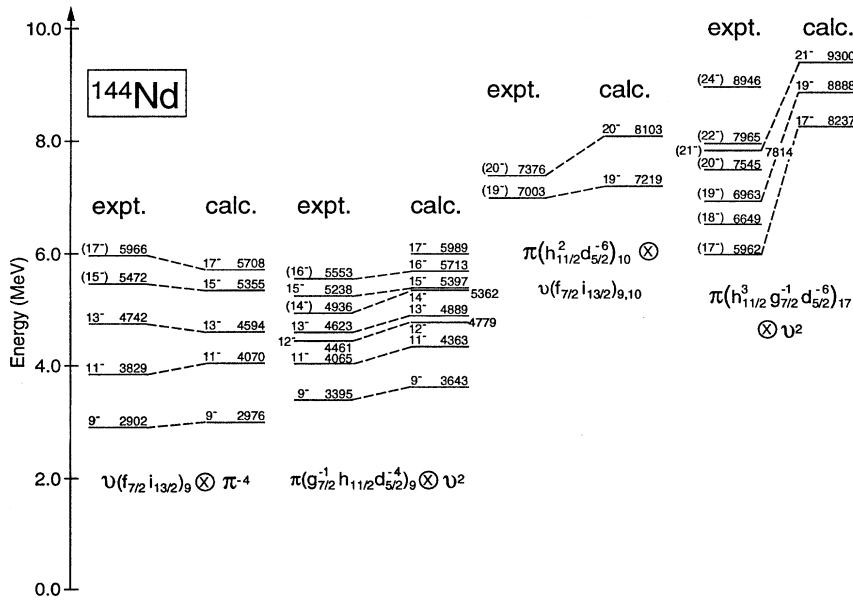


FIG. 6. A comparison of calculated and observed energy levels for ^{144}Nd .

5238, and 5553 keV. An empirical shell-model calculation for the $[\pi(g_{7/2}^{-1}h_{11/2}d_{5/2}^{-4})\nu(f_{7/2}^2)]_9$ configuration yields an energy of 3643 keV, which is close to the 3395 keV energy observed for the 9_2^- state. In addition, the $J=11-17$ members of this sequence can be understood in terms of the coupling of the $\pi(g_{7/2}^{-1}h_{11/2}d_{5/2}^{-4})$ proton configuration to $\nu(f_{7/2}^2)$ neutron couplings. The results of empirical shell-model calculations for these configurations are shown in Fig. 6. The calculations reproduce the data well [to better than 320 keV for all but the (14^-) state, for which the agreement is within 426 keV]. While the empirical shell-model calculations for these states yield good agreement with the data, there is another possibility for the configuration of the 5962 keV (17^-) state, which is discussed below.

States involving the coupling of two $h_{11/2}$ protons to $J=10$ are also known to occur near the yrast line (for example, see [1]). Using the method of the empirical shell model, we have calculated that the $[\pi(h_{11/2}^2d_{5/2}^{-6})\nu(f_{7/2}i_{13/2})]_{19,20}$ states should occur at 7219 and 8103 keV for $J=19$ and 20 , respectively. There are (19^-) and (20^-) states observed at 7003 and 7376 keV, respectively, which decay to the $\nu(f_{7/2}i_{13/2})$ sequence, and we conclude that these are the $[\pi(h_{11/2}^2d_{5/2}^{-6})\nu(f_{7/2}i_{13/2})]_{19,20}$ states. While the disparity between the observed and calculated energies for the 20^- state is troubling, the transition between these two states supports such an interpretation.

Piiparinen *et al.* [20] proposed that a 24^- state at 8640 keV in the $N=84$ isotope ^{148}Gd has the $[\pi(h_{11/2}^3d_{5/2}^{-3})\nu(f_{7/2}h_{9/2})]$ configuration. We have tentatively located a state of the same spin and parity at 8946 keV, and have proposed previously [4] that this state also has a configuration involving three $h_{11/2}$ protons: $\pi(h_{11/2}^3g_{7/2}^{-1})\nu(f_{7/2}h_{9/2})$. Since this unusual proton configuration can also couple to other neutron configurations of lower spins, it is natural to look in the level scheme for a sequence of states that corresponds to the coupling of the $\pi(h_{11/2}^3g_{7/2}^{-1})$ proton configuration to lower spin $f_{7/2}^2$ neutron configurations. Such couplings should result

in a sequence of negative-parity states with $J=17-23$. In addition, the coupling of this proton configuration to the stretched $\nu(f_{7/2}h_{9/2})_8$ neutron configuration should yield a 25^- state. The states in this sequence should be connected by $E2$ transitions which are comparable to those in the ground-state sequence of ^{148}Gd as well as significant $M1$ transitions. Such a sequence appears to occur, and includes the 5962, 6649, 6963, 7545, 7814, and 7965 keV states.

Since this sequence of states could be described as a proton configuration coupled to the two-neutron states of the ground-state sequence of ^{148}Gd , it would be expected that the spacings between the states in this high-spin sequence in ^{144}Nd would be similar to those in the ground-state sequence of ^{148}Gd . The similarity of the spacings of the two sequences, as shown in [4], supports this interpretation. This possible $\pi(h_{11/2}^3g_{7/2}^{-1})_{17}$ sequence does *not* include either a 23^- state or a 25^- state. The 23^- state may occur at an energy close to or above the 8946 keV (24^-) state, and may not be populated as a result. A more sensitive experiment may be necessary to locate both the 23^- and 25^- members of this sequence.

One additional problem is that the apparent 17^- member of the $\pi(h_{11/2}^3g_{7/2}^{-1})$ sequence at 5962 keV can also plausibly be interpreted as a member of the $\pi(g_{7/2}^{-1}h_{11/2}d_{5/2}^{-4})$ sequence, as discussed above. It is possible that the 5962 keV state is a mixture of both configurations, and it seems likely that it also mixes with the tentatively assigned $\nu(f_{7/2}i_{13/2})$ 17^- state at 5966 keV.

We performed empirical shell-model calculations for the $J=17, 19$, and 21 states in the possible $\pi(h_{11/2}^3g_{7/2}^{-1})$ sequence, and these results do *not* support this interpretation. These calculations relied on MPME's from ^{151}Ho , which were extracted from Ref. [21]. Since the corresponding MPME's necessary for calculation of the even-spin states were not available, we did not calculate them. As illustrated in Fig. 6, the calculated energies for these three states are between 1.5 and 2.3 MeV higher than the energies observed.

In light of these results, the origin of this sequence is not at all clear. Several avenues of inquiry could be followed toward understanding this sequence. First, it is possible that these states do *not* have negative parity. A conversion-electron- γ -ray coincidence experiment could be used to investigate this question. Second, this sequence could arise from a configuration involving an octupole phonon, which we have not considered in detail at high spins. Third, the determination of the MPME's relies on the accuracy of the configuration assignments given in other nuclei. It may be that one or more of these assignments is incorrect, and that some of the MPME's are also incorrect as a result.

VI. SUMMARY

The near-yrast spectrum of the $N=84$ isotope ^{144}Nd has been studied using the $^{130}\text{Te}(^{18}\text{O},4n)$ reaction at a lab energy of 85 MeV with the Florida State University-University of Pittsburgh γ ray array. Sixteen new states and 23 new γ rays

were placed in the level scheme. We have been able to interpret most of the yrast and near-yrast negative-parity states in terms of shell-model configurations involving the valence nucleons using empirical shell-model calculations. However, the interpretation of a sequence of states from $J=17-24$ in terms of the $\pi(h_{11/2}^3 g_{7/2}^{-1})$ proton configuration coupled to $f_{7/2}^2$ and $f_{7/2} h_{9/2}$ neutron configurations is problematic because the observed energies cannot be satisfactorily reproduced with empirical shell-model calculations. The firm determination of parities is clearly important to fully understanding this nucleus, and a high-efficiency conversion-electron- γ -ray coincidence experiment might allow their measurement.

ACKNOWLEDGMENTS

This work was supported by the National Science Foundation and the State of Florida.

-
- [1] T. Glasmacher, D.D. Caussyn, P.D. Cottle, J.W. Holcomb, T.D. Johnson, K.W. Kemper, M.A. Kennedy, and P.C. Womble, *Phys. Rev. C* **47**, 2586 (1993).
- [2] P.D. Cottle, S.M. Aziz, J.D. Fox, K.W. Kemper, and S.L. Tabor, *Phys. Rev. C* **40**, 2028 (1989).
- [3] D.D. Caussyn, S.M. Aziz, P.D. Cottle, T. Glasmacher, and K.W. Kemper, *Phys. Rev. C* **43**, 2098 (1991).
- [4] J.K. Jewell, O.J. Tekyi-Mensah, P.D. Cottle, J. Döring, P.V. Green, J.W. Holcomb, G.D. Johns, J.L. Johnson, T.D. Johnson, K.W. Kemper, P.L. Kerr, S.L. Tabor, P.C. Womble, and V.A. Wood, *Z. Phys. A* **348**, 69 (1994).
- [5] L. Bargioni, P.G. Bizzeti, A.M. Bizzeti-Sona, D. Bazzacco, S. Lunardi, P. Pavan, C. Rossi-Alvarez, G. de Angelis, G. Maron, and J. Rico, *Phys. Rev. C* **51**, R1057 (1995).
- [6] I. Talmi, *Rev. Mod. Phys.* **34**, 704 (1962).
- [7] A. Ercan, R. Broda, P. Kleinheinz, M. Piiparinen, R. Julin, and J. Blomqvist, *Z. Phys. A* **329**, 63 (1988).
- [8] M. Piiparinen, Y. Nagai, P. Kleinheinz, M.C. Bosca, B. Rubio, M. Lach, and J. Blomqvist, *Z. Phys. A* **338**, 417 (1991).
- [9] A. Kuhnert, D. Alber, H. Grawe, H. Kluge, K.H. Maier, W. Reviol, X. Sun, E.M. Beck, A.P. Byrne, H. Hübel, J.C. Bacelar, M.A. Deleplanque, R.M. Diamond, and F.S. Stephens, *Phys. Rev. C* **46**, 484 (1992).
- [10] M. Piiparinen, P. Kleinheinz, S. Lunardi, M. Ogawa, G. de Angelis, F. Soramel, W. Meczynski, and J. Blomqvist, *Z. Phys. A* **337**, 387 (1990).
- [11] E. Newman, K.S. Toth, R.L. Auble, R.M. Gaedke, M.F. Roche, and B.H. Wildenthal, *Phys. Rev. C* **1**, 1118 (1970).
- [12] B.H. Wildenthal, E. Newman, and R.L. Auble, *Phys. Rev. C* **3**, 1199 (1971).
- [13] H.J. Scheerer, D. Pereira, A. Chalupka, R. Gyufko, and C.-A. Wiedner, *Z. Phys. A* **308**, 183 (1982).
- [14] C.F. Liang, P. Paris, P. Kleinheinz, B. Rubio, M. Piiparinen, D. Schardt, A. Plochocki, and R. Barden, *Phys. Lett. B* **191**, 245 (1987).
- [15] E. Newman, K.S. Toth, D.C. Hensley, and W.D. Schmidt-Ott, *Phys. Rev. C* **9**, 674 (1974).
- [16] P. Kleinheinz, M.R. Maier, R.M. Diamond, F.S. Stephens, and R.K. Sheline, *Phys. Lett.* **53B**, 442 (1975).
- [17] J.K. Tuli, *Nucl. Data* **56**, 607 (1989).
- [18] S.J. Robinson, J. Jolie, H.G. Börner, P. Schillebeeckx, S. Ulbig, and K.P. Lieb, *Phys. Rev. Lett.* **73**, 412 (1994).
- [19] P.D. Cottle, K.W. Kemper, M.A. Kennedy, L.K. Fifield, and T.R. Ophel, *Phys. Rev. C* **47**, 1048 (1993).
- [20] M. Piiparinen, M.W. Drigert, R.V.F. Janssens, I. Ahmad, J. Borggreen, R.R. Chasman, P.J. Daly, B.K. Dichter, H. Emling, U. Garg, Z.W. Grabowski, R. Holzmann, T.L. Khoo, W.C. Ma, M. Quader, D.C. Radford, and W. Trzaska, *Phys. Lett. B* **194**, 468 (1987).
- [21] J. Gizon, A. Gizon, S. Andre, J. Genevey, J. Jastrzebski, R. Kossakowski, M. Moszynski, and Z. Preibisz, *Z. Phys. A* **301**, 67 (1981).